



## Effect of deuteration on some structural parameters of methyl groups in proteins as evaluated by residual dipolar couplings

Anthony Mittermaier<sup>a</sup> & Lewis E. Kay<sup>a,b</sup>

<sup>a</sup>Department of Biochemistry, University of Toronto, Toronto, Ontario, Canada M5S 1A8; <sup>b</sup>Protein Engineering Network Centres of Excellence and Departments of Medical Genetics and Chemistry, University of Toronto, Toronto, Ontario, Canada M5S 1A8

Received 9 January 2002; Accepted 1 March 2002

**Key words:** deuteration, methyl group dynamics, methyl group structure, residual dipolar couplings, spin relaxation

### Abstract

One bond methyl  $^1\text{H}$ - $^{13}\text{C}$  and  $^{13}\text{C}_{\text{methyl}}$ - $^{13}\text{C}$  scalar and residual dipolar couplings have been measured at sites in an  $^{15}\text{N}$ ,  $^{13}\text{C}$ ,  $\sim 50\%$   $^2\text{H}$  labeled sample of the B1 immunoglobulin binding domain of peptostreptococcal protein L to investigate changes in the structure of methyl groups in response to deuterium substitution. Both one bond methyl  $^1\text{H}$ - $^{13}\text{C}$  and  $^{13}\text{C}_{\text{methyl}}$ - $^{13}\text{C}$  scalar coupling constants have been found to decrease slightly with increasing deuterium content. Previous studies have shown that  $^1\text{H}$ - $^{13}\text{C}$  couplings in methyl groups are exquisitely sensitive to electronic structure, with decreases in coupling values as a function of deuteration consistent with a slight lengthening of the remaining H-C bonds. Changes in the  $\text{H}_{\text{methyl}}\text{C}_{\text{methyl}}\text{C}$  angle are found to be small, with average differences on the order of  $0.3 \pm 0.1^\circ$  and  $0.4 \pm 0.2^\circ$  between  $\text{CH}_3$ ,  $\text{CH}_2\text{D}$  and  $\text{CH}_3$ ,  $\text{CHD}_2$  isotopomers, respectively. Knowledge of methyl geometry is a prerequisite for the extraction of accurate dynamics parameters from spin relaxation studies involving these groups.

### Introduction

Methyl groups are particularly valuable probes of molecular motion. For example, they are distributed quite uniformly throughout many protein sequences and are often present at intermolecular interfaces, binding sites and core protein positions (Janin et al., 1988). Hence a study of their dynamics can provide a comprehensive picture of motion throughout the molecule. In addition, they are extremely attractive reporter groups because they possess uniquely favorable spectroscopic properties (Kay et al., 1992). Interpretation of methyl  $^{13}\text{C}$  relaxation rates measured in samples that are fully protonated is complicated, however, by intra-methyl  $^1\text{H}$ - $^{13}\text{C}$  dipolar cross-correlated relaxation (Kay et al., 1992; Palmer et al., 1991). With this limitation in mind, several different approaches have been developed for using methyls to study sidechain dynamics. In one method,  $^2\text{H}$  spin relaxation properties of  $^{13}\text{CH}_2\text{D}$  methyl isotopomers are measured in  $^{13}\text{C}$  labeled and fractionally deuterated proteins

(Muhandiram et al., 1995). In a second approach  $^{13}\text{C}$  auto-relaxation rates of  $^{13}\text{CHD}_2$  methyl isotopomers are obtained (Ishima et al., 2001; LeMaster & Kushlan, 1996). In this case,  $^1\text{H}$ - $^{13}\text{C}$  dipole-dipole cross-correlated spin relaxation effects are eliminated since only a single  $^1\text{H}$ - $^{13}\text{C}$  spin pair is present in each methyl. More recently, our laboratory has developed experiments for studying  $^1\text{H}$ - $^{13}\text{C}$  dipole-dipole cross-correlated spin relaxation in methyls of the  $^{13}\text{CH}_2\text{D}$  variety. It is clear that depending on the application, different methyl isotopomers will prove advantageous.

Correct interpretation of relaxation data from methyl groups in terms of dynamics presupposes that certain geometrical constants are known to good accuracy. For example, in the study of  $^2\text{H}$  spin relaxation the angle between the unique axis of the  $^2\text{H}$  quadrupolar tensor and the methyl rotation axis must be available as well as the magnitude of the quadrupolar coupling constant,  $e^2qQ/h$  (Mittermaier and Kay, 1999; Muhandiram et al., 1995). In a similar manner, in the analysis of  $^{13}\text{C}$  relaxation data recorded on

methyl groups, both the methyl  $^1\text{H}$ - $^{13}\text{C}$  bond length and the angle between this bond and the methyl averaging axis must be known (Nicholson et al., 1992). Recently our laboratory has shown that  $^2\text{H}$  quadrupolar coupling ‘constants’ are uniform in proteins by accurately measuring  $^2\text{H}$  quadrupolar couplings at methyl sites in a protein that was oriented in solution (Mittermaier & Kay, 1999). Assuming an angle of  $109.5^\circ$  between the principal axis of the quadrupolar tensor and the methyl three-fold axis, an average value of  $167 \pm 1$  kHz is obtained for the quadrupolar coupling constant (Mittermaier and Kay, 1999). Ottiger and Bax (1999) have used the protein ubiquitin dissolved in dilute liquid crystalline media to measure the effective CH bond length ( $r_{\text{CH}}$ ) and HCC bond angle ( $\beta$ ) in  $\text{CH}_3$  methyls. A value of  $-0.228 \pm 0.002 \text{ \AA}^{-3}$  was obtained for the product  $\langle P_2(\cos \beta) \cdot r_{\text{CH}}^{-3} \rangle$  where  $P_2(x) = (3x^2 - 1)/2$  and the angular brackets,  $\langle \rangle$ , are used to indicate time-averaging. Although independent values for these parameters cannot be extracted by this method, the analysis of relaxation data is fairly insensitive to the particular choice of  $P_2(\cos \beta)$  and  $r_{\text{CH}}^{-3}$  so long as their product is constant (Ishima et al., 2001).

Since deuterium and hydrogen are electronically equivalent, CD and CH bonds possess identical energy surfaces. However, the asymmetry of the potential surface and the mass difference between  $^1\text{H}$  and  $^2\text{H}$  atoms results in time-averaged geometries that show isotopic dependence. Energy surfaces may be constructed for small molecules (less than approximately 10 atoms) from which vibrational and rotational modes are extracted along with average values of physical properties. In a study of methane and its deuterated analogs, small changes in ( $r_{\text{CH}}$ ) and ( $\beta$ ) were observed with increasing deuterium substitution (Raynes et al., 1988). Unfortunately, this computational approach cannot be applied in a completely rigorous manner to the study of methyl group structure in the complex environment of a protein. Moreover, it is not *a priori* clear that these results can be directly transferred to methyl groups in other molecules. Knowledge of how  $\beta$  changes with deuteration is particularly important in relaxation studies of different methyl isotopomers since the extracted dynamics parameters can be quite sensitive to  $\beta$  for values in the neighborhood of  $110^\circ$ .

With this in mind we have carried out a study similar to that of Ottiger and Bax in which  $\langle P_2(\cos \beta) \cdot r_{\text{CH}}^{-3} \rangle$  has been measured for  $\text{CH}_3$ ,  $\text{CH}_2\text{D}$  and  $\text{CHD}_2$  methyl groups in a single random fractionally deuter-

ated protein sample. The results show several very small differences among the isotopomers that are consistent with minute changes in methyl group geometry. First, a decrease in  $^1J_{\text{CH}}$  was observed with increasing levels of deuteration (i.e.,  $^1J_{\text{CH}}^{\text{CH}_3} > ^1J_{\text{CH}}^{\text{CH}_2\text{D}} > ^1J_{\text{CH}}^{\text{CHD}_2}$ ), showing the same trend seen in experimental (Bennett et al., 1989) and *ab initio* (Wigglesworth et al., 1997) investigations of methane. In addition, very slight differences in values of  $\langle P_2(\cos \beta) \cdot r_{\text{CH}}^{-3} \rangle$  were found for the three methyl types, although with low statistical significance (p values ranging from 5% to 28%). This study demonstrates the high sensitivity of scalar and dipolar couplings to minute changes in structure.

## Materials and methods

### Sample preparation

Samples of  $^{15}\text{N}$ ,  $^{13}\text{C}$ ,  $\sim 50\%$  randomly  $^2\text{H}$  labeled B1 domain of protein L (64 amino acids) with a Y45W mutation were prepared as described previously (Mittermaier and Kay, 2001). NMR experiments were performed on 1.8 mM protein samples containing 50 mM  $\text{Na}_3\text{PO}_4$  pH 6.0, 0.05%  $\text{NaN}_3$  and 10%  $^2\text{H}_2\text{O}$  at  $25^\circ\text{C}$  using a Varian Inova spectrometer operating at 600 MHz  $^1\text{H}$  frequency. In cases where sample alignment was required Pfl bacteriophage (Hansen et al., 1998) was added to samples described above to give a final concentration of  $19 \text{ mg ml}^{-1}$ .

### Data acquisition and analysis

$^{13}\text{C}_{\text{methyl}}\text{-}^{13}\text{C}$  dipolar couplings were measured for  $^{13}\text{CH}_3$ ,  $^{13}\text{CH}_2\text{D}$  and  $^{13}\text{CHD}_2$  methyls by selection of the appropriate isotopomer during the course of the pulse sequence. The scheme for  $^{13}\text{CH}_2\text{D}$  selection has been described previously (Mittermaier and Kay, 1999). Combined selection of  $^{13}\text{CH}_3$  and  $^{13}\text{CHD}_2$  isotopomers was achieved using a variant of the scheme for  $^{13}\text{CH}_2\text{D}$  selection whereby the receiver phase is not alternated when the phase of the proton pulse for isotopomer selection is inverted (phase  $\phi_2$  in Figure 1a of Mittermaier and Kay (1999)). Experiments for measuring one-bond  $^1\text{H}_{\text{methyl}}\text{-}^{13}\text{C}_{\text{methyl}}$  dipolar couplings in each of the three methyl isotopomers are illustrated in Figure 1 of this paper.

$^{13}\text{C}_{\text{methyl}}\text{-}^{13}\text{C}$  ( $^1\text{H}_{\text{methyl}}\text{-}^{13}\text{C}_{\text{methyl}}$ ) dipolar couplings were obtained from sets of 15 (16) constant-time  $^1\text{H}$ - $^{13}\text{C}$  correlation spectra recorded with spectral widths of 9000.9 and 3600.0 Hz, and 576 and

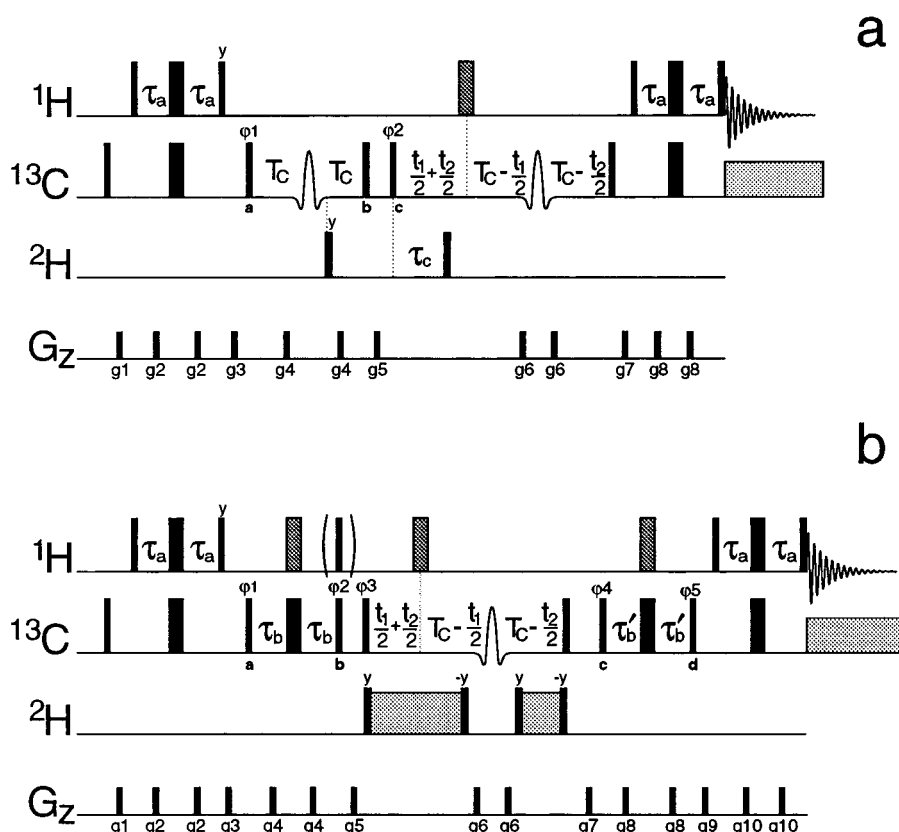


**Figure 1.** Pulse schemes used to measure  $^1\text{H}_{\text{methyl}}-^{13}\text{C}_{\text{methyl}}$  dipolar couplings with selection for (a)  $\text{CH}_3$  and (b)  $\text{CH}_2\text{D}$  or  $\text{CHD}_2$  methyl groups (see below). All narrow (wide) pulses are applied with a flip angle of  $90^\circ$  ( $180^\circ$ ). The  $^1\text{H}$ ,  $^{13}\text{C}$  and  $^2\text{H}$  carriers are positioned at 4.73 (water), 20 and 1 ppm. All  $^1\text{H}$  pulses are applied with a field strength of 31 kHz with composite inversion pulses ( $90_x180_y90_x$ ) (Freeman et al., 1980) indicated by shading. All  $^{13}\text{C}$  pulses employ a 19 kHz field with the exception of the shaped pulses which have a REBURP profile (Geen & Freeman, 1991) ( $400 \mu\text{s } 180^\circ$  centered at 35 ppm) and the 2.6 kHz WALTZ16 (Shaka et al., 1983) decoupling field applied during acquisition. The  $^2\text{H}$   $90^\circ$  pulses employ a field strength of 2.0 kHz except for the 640 Hz WALTZ16 $_x$  decoupling train. The delays used are  $\tau_a = 1.7$  ms;  $\tau_b = 1.97$  ms;  $\tau'_b = 1.81$  ms;  $T_C = 14.5$  ms. Quadrature detection in the  $^{13}\text{C}$  dimension is achieved with States-TPPI (Marion et al., 1989) of  $\phi_2$  in (a) and  $\phi_3$  in (b). The phase cycle employed in (a) is  $\phi_1 = 2(x), 2(-x)$ ;  $\phi_2 = x, -x$ ; rec =  $x, -x, -x, x$ ; (b)  $\phi_1 = x, -x$ ;  $\phi_3 = 2(x), 2(-x)$ ;  $\phi_4 = 4(x), 4(-x)$ ; rec =  $x, -x, -x, x, -x, x, x, -x$ . The values of  $\phi_2$  and  $\phi_5$  are set to  $x$  ( $y$ ) when selection of  $\text{CH}_2\text{D}$  ( $\text{CHD}_2$ ) methyls is desired and the  $^1\text{H}$   $90^\circ$  pulse in parenthesis is omitted (applied). The gradients used in (a) are  $g_1 = 0.5$  ms, 5 G/cm;  $g_2 = 0.3$  ms, 3 G/cm;  $g_3 = 1.5$  ms, 15 G/cm;  $g_4 = 0.1$  ms, 10 G/cm;  $g_5 = 0.25$  ms, 10 G/cm;  $g_6 = 0.2$  ms, 10 G/cm;  $g_7 = 0.5$  ms, 15 G/cm;  $g_8 = 0.3$  ms, 2 G/cm and in (b)  $g_1 = 0.5$  ms, 5 G/cm;  $g_2 = 0.3$  ms, 3 G/cm;  $g_3 = 1.5$  ms, 15 G/cm;  $g_4 = 0.3$  ms, 12 G/cm;  $g_5 = 1$  ms, 8 G/cm;  $g_6 = 0.2$  ms, 10 G/cm;  $g_7 = 0.5$  ms, 15 G/cm;  $g_8 = 0.3$  ms, 6 G/cm;  $g_9 = 0.5$  ms, 10 G/cm;  $g_{10} = 0.3$  ms, 2 G/cm.

102 complex points in the direct and indirect dimensions, respectively. Eight scans were recorded/FID along with a relaxation delay of 1.5 s to give a net acquisition time of 0.7 h/spectrum. Mirror image linear prediction was applied to the  $^{13}\text{C}$  dimension (Zhu and Bax, 1990), both dimensions were apodized with shifted sine bell window functions, zero-filled to  $2048 \times 512$  complex points and Fourier transformed, using the NMRPipe/NMRdraw suite of programs (Delaglio et al., 1995). Peak volumes were fit using nlinLS software (Delaglio et al., 1995).  $^{13}\text{C}_{\text{methyl}}-^{13}\text{C}$  coupling delays, corresponding to **T** in Figure 1a in

Mittermaier and Kay (1999), were: [0, 5, 10, 15, 20, 25, 30, 35, 40, 45, 50, 55, 60, 65, 70] ms. Coupling delays ( $t_1$  in Figure 1a,b) of [0.00, 1.8, 3.6, 5.5, 7.3, 9.1, 10.9, 12.7, 14.6, 16.4, 18.2, 20.0, 21.8, 23.6, 25.5, 27.3] ms were employed in all  $^1\text{H}_{\text{methyl}}-^{13}\text{C}_{\text{methyl}}$  coupling experiments.

$^{13}\text{C}_{\text{methyl}}-^{13}\text{C}$  coupling values,  $^1J_{\text{CC}} + ^1D_{\text{CC}}$ , (where  $^1D_{\text{CC}}$  is the one-bond carbon-carbon dipolar coupling,  $^1D_{\text{CC}} = 0$  in the absence of alignment) were extracted from the time dependence of cross-peak intensities by non-linear least-squares fitting of a time

modulation function,

$$I(\mathbf{T}) = [c_1 \cdot \cos\{\pi \cdot ({}^1J_{CC} + {}^1D_{CC}) \cdot \mathbf{T}\} + c_2] \exp\{-(c_3 \mathbf{T})^2\}, \quad (1)$$

where  $I(\mathbf{T})$  is the intensity of a cross-peak obtained with coupling delay  $\mathbf{T}$ . The coefficients  $c_1$ ,  $c_2$  and  $c_3$  are fit simultaneously with  $({}^1J_{CC} + {}^1D_{CC})$  and account for overall scaling of the data, incomplete non-methyl  ${}^{13}\text{C}$  inversion during the constant-time period and multiple long-range  ${}^{13}\text{C}_{\text{methyl}}$  homonuclear couplings (Ottiger et al., 1998), respectively.  ${}^1\text{H}$ - ${}^{13}\text{C}$  couplings in the  $\text{CH}_3$  selective experiment of Figure 1a were obtained by fitting cross-peak intensities to a time modulation function of the form,

$$I(t_1) = [c_1 \cdot \cos\{3\pi \cdot ({}^1J_{\text{CH}} + {}^1D_{\text{CH}}) \cdot t_1\} + c_2 \cdot \cos\{\pi \cdot ({}^1J_{\text{CH}} + {}^1D_{\text{CH}}) \cdot t_1\}] \exp\{-(c_3 \cdot t_1)^2\}, \quad (2)$$

where  $c_1 = 3c_2$  in the absence of cross-correlated spin relaxation and  $c_3$  accounts for multiple long range  ${}^1\text{H}$ - ${}^{13}\text{C}_{\text{methyl}}$  couplings. In the  $\text{CH}_2\text{D}$  and  $\text{CHD}_2$  selective experiments of Figure 1b  ${}^1\text{H}$ - ${}^{13}\text{C}$  couplings were obtained using a fitting function,

$$I(t_1) = [c_1 \cdot \cos\{n\pi \cdot ({}^1J_{\text{CH}} + {}^1D_{\text{CH}}) \cdot t_1\} + c_2] \exp\{-(c_3 \cdot t_1)^2\}, \quad (3)$$

where  $n = 1, 2$  for  $\text{CHD}_2$  and  $\text{CH}_2\text{D}$  methyls, respectively. As before, the parameter  $c_1$  scales the data, while  $c_2$  takes into account incomplete  ${}^1\text{H}$  inversion due to imperfections in the  ${}^1\text{H}$   $180^\circ$  pulse applied at time  $t_1/2 + t_2/2$  during the constant-time period. The definition of  $c_3$  is as in Equation 2. All minimizations were performed using the MATLAB software package.

The majority of measurements were repeated at least twice to obtain an estimate of random errors. In the case of measurement of  ${}^1\text{H}$ - ${}^{13}\text{C}$  couplings, two identical experiments were performed in the absence of aligning media for each of the isotopomer types, three experiments were recorded in the presence of phase selecting for either  $\text{CH}_2\text{D}$  or  $\text{CHD}_2$  isotopomers, while four data sets were obtained with selection for  $\text{CH}_3$  methyls. Values of  ${}^1J_{\text{CH}} + {}^1D_{\text{CH}}$  were found to be highly reproducible with rmsds between data sets on the order of 1% of the total range of values ( $\approx 0.15$  Hz).  ${}^{13}\text{C}_{\text{methyl}}$ - ${}^{13}\text{C}$  couplings from  $\text{CH}_2\text{D}$  methyl groups were obtained from duplicate experiments recorded on both aligned and unaligned samples, while for  $\text{CH}_3/\text{CHD}_2$  methyls, only a single data set was obtained for each sample. Although

${}^{13}\text{C}_{\text{methyl}}$ - ${}^{13}\text{C}$  scalar coupling values have an isotope dependence discussed later in the text, carbon-carbon dipolar couplings showed no systematic deviation between the methyl isotopomers.  ${}^{13}\text{C}_{\text{methyl}}$ - ${}^{13}\text{C}$  dipolar couplings were therefore calculated as the mean of values derived from  $\text{CH}_3$  and  $\text{CH}_2\text{D}$  isotopomers; couplings obtained from  $\text{CHD}_2$  methyls were not included in the average because of the larger error associated with these values due to the small population of  $\text{CHD}_2$  isotopomer in our sample.

#### Data and statistical analysis

Differences in  ${}^1J_{\text{CH}}$  and  ${}^1J_{\text{CC}}$  values between isotopomer types were calculated for each methyl group to yield mean differences in scalar coupling constants,  $\langle \Delta {}^1J_{\text{CH}} \rangle$  and  $\langle \Delta {}^1J_{\text{CC}} \rangle$ . The standard errors of  $\langle \Delta {}^1J_{\text{CH}} \rangle$  and  $\langle \Delta {}^1J_{\text{CC}} \rangle$  were taken to be  $s/\sqrt{N}$  where  $s$  is the standard deviation of the  $\Delta {}^1J_{\text{CH}}$  or  $\Delta {}^1J_{\text{CC}}$  values and  $N$  is the number of methyl groups included in the analysis (30). Assuming that errors in  $\langle \Delta {}^1J_{\text{CH}} \rangle$  and  $\langle \Delta {}^1J_{\text{CC}} \rangle$  are distributed normally, only 1% of the time will values lie outside the bounds given by  $\langle \Delta {}^1J \rangle \pm t_{0.01} s/\sqrt{N}$ , thus defining the 99% confidence regions. For 29 degrees of freedom,  $t_{0.01} = 2.756$ .

The statistical significance of differences in  $\langle \Delta {}^1J_{\text{CH}} \rangle$  and  $\langle \Delta {}^1J_{\text{CC}} \rangle$  from zero was calculated by evaluating

$$p = \mathbf{I}_{\frac{N-1}{N-1+p^2}} \left( \frac{N-1}{2}, \frac{1}{2} \right), \quad (4)$$

where  $p$  is the probability that a sample of size  $N$  and mean deviating from zero by an amount  $\langle \Delta {}^1J_{\text{Cj}} \rangle$ ,  $j = \text{H, C}$ , or greater could be drawn from a population with a mean of zero and standard deviation estimated by the sample standard deviation,  $s$  (Zar, 1984a). In Equation [4]  $t$  is given by,

$$t = \frac{\langle {}^1J_{\text{CH}} \rangle}{s/\sqrt{N}} \text{ or } t = \frac{\langle \Delta {}^1J_{\text{CC}} \rangle}{s/\sqrt{N}} \quad (5)$$

and  $\mathbf{I}$  is the incomplete beta function. Note that very small  $p$  values imply that the sample of  $\Delta {}^1J_{\text{CH}}$  or  $\Delta {}^1J_{\text{CC}}$  values could not reasonably be obtained from a population of mean zero and hence that there are differences in scalar couplings between the pair of isotopomers that are under examination.

Values of  $\langle P_2(\cos\beta) \cdot r_{\text{CH}}^{-3} \rangle$  for each of the isotopomers were obtained following the approach of Ottiger and Bax (1999).  ${}^1D_{\text{CH},i}$  vs.  ${}^1D_{\text{CC},i}$  correlations for  $\text{CH}_3$ ,  $\text{CH}_2\text{D}$  and  $\text{CHD}_2$  methyls were fit to straight lines through the origin with slopes,  $m$ , minimizing a

target function (Press et al., 1988)

$$\chi_m^2 = \sum ({}^1D_{CH,i} - m \cdot {}^1D_{CC,i})^2 / \{\sigma_{CH,i}^2 (1 + \rho_i^2 \cdot m^2)\}, \quad (6)$$

where the summation over  $i$  includes all methyl groups of a particular isotopomer,  $\sigma_{CH,i}$  and  $\sigma_{CC,i}$  are the standard errors in  ${}^1D_{CH,i}$  and  ${}^1D_{CC,i}$ , respectively, and  $\rho_i = \sigma_{CC,i}/\sigma_{CH,i}$ . Uncertainty in the value of  $\beta$  for each isotopomer may be evaluated using standard methods. However, due to the fact that all three comparisons share the same set of  ${}^1D_{CC}$  data, the errors in  $\beta_{CH_3}$ ,  $\beta_{CH_2D}$ , and  $\beta_{CHD_2}$  cannot be considered independent, complicating the analysis of uncertainties in  $\Delta\beta$ .

In order to estimate errors in  $\beta$  values we have used a bootstrap simulation protocol (Efron & Tibshirani, 1986). In this approach, the experimental sample of 30  ${}^1D_{CC}$ ,  ${}^1D_{CH}^{CH_3}$ ,  ${}^1D_{CH}^{CH_2D}$  and  ${}^1D_{CH}^{CHD_2}$  values is assumed to approximate the universe of possible values. This experimental sample is, in turn, approximated by a bootstrap sample, constructed by randomly selecting 30 sets of  ${}^1D_{CC}$ ,  ${}^1D_{CH}^{CH_3}$ ,  ${}^1D_{CH}^{CH_2D}$  and  ${}^1D_{CH}^{CHD_2}$  values from the methyl groups in the experimental sample such that data from a given methyl group may be included more than once. (Note that if each methyl is selected the bootstrap and the experimental samples are identical). Values of  $\Delta\beta$  are calculated for the bootstrap sample and compared with values for the experimental sample. If a bootstrap value is larger than the experimental one by a certain amount then it is assumed that the experimental value may, correspondingly, be larger than the true value by the same amount. Distribution functions,  $f(\Delta\beta)$  for the true values of  $\Delta\beta$  were thus calculated from  $10^5$  bootstrap iterations.

In fits according to Equation [6] it was found that estimates of  $\sigma_{CC}$  and  $\sigma_{CH}$  from duplicate experiments were too small, judging by reduced  $\chi_m^2$  values of greater than 15. Since the slopes of the  ${}^1D_{CH,i}$  vs.  ${}^1D_{CC,i}$  correlations (see above) have a small but non-negligible ( $\leq 1\%$ ) dependence on  $\rho$ , whose true value is not known, we have chosen to propagate the uncertainty in  $\rho$  into the uncertainties in the slopes by varying  $\rho$  in the bootstrap simulations. A value of  $\rho$  was therefore selected randomly in each bootstrap calculation such that  $\rho = 10^\lambda$  and  $\lambda$  is uniformly distributed between  $-2$  and  $2$ . The values of  $\Delta\beta$  used to compare with the bootstrap values (referred to as experimental values above) were taken as the means of all 100 000 bootstrap values.

An alternative approach has also been used to evaluate whether values of  ${}^1D_{CH}$  obtained from each of

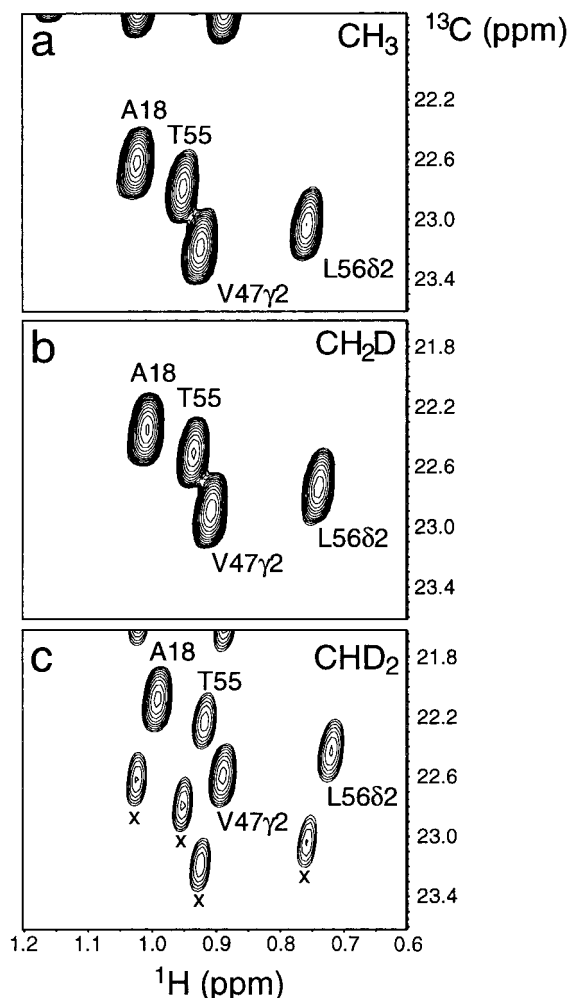


Figure 2. Regions of  ${}^1H$ - ${}^{13}C$  correlation spectra of the B1 domain of protein L recorded at 600 MHz ( ${}^1H$  frequency) in isotropic solution using the pulse schemes of (a) Figure 1a, (b) Figure 1b ( $\varphi_2 = \varphi_5 = x$ , bracketed pulse omitted) and (c) Figure 1b ( $\varphi_2 = \varphi_5 = y$ , bracketed pulse included) with the delay  $t_1$  set to 0. Residue labels are according to the numbering convention of Scalley et al. (1997). In (c), peaks corresponding to the  $CH_3$  isotopomer of each methyl group are indicated with (x).

the three methyl isotopomers are different. In this approach couplings from the pair of isotopomers under consideration are plotted and a slope,  $m$ , obtained from standard linear regression, assuming that the correlation goes through the origin (i.e., zero intercept). Defining  $t$  as  $t = (1 - m)/s_m$  where  $s_m$  is the standard error in  $m$ , the probability that a value of  $t$  as large or larger than the one calculated could be obtained if the data sets considered are the same is  $p/2$ , with  $p$  defined in Equation 4 (Zar, 1984b). Low values of  $p$  again indicate that the two data sets are unique.

## Results and discussion

Recently Ottiger and Bax (1999) have described a set of experiments to measure one bond  $^{13}\text{C}_{\text{methyl}}\text{-}^{13}\text{C}$  ( $^1\text{D}_{\text{CC}}$ ) and  $^1\text{H}_{\text{methyl}}\text{-}^{13}\text{C}_{\text{methyl}}$  ( $^1\text{D}_{\text{CH}}$ ) dipolar couplings in proteins dissolved in dilute liquid crystalline media (Ottiger and Bax, 1999; Ottiger et al., 1998). These workers went on to show that so long as CH bond vibrations and librations are assumed to be uncorrelated with CC bond stretching a plot of  $^1\text{D}_{\text{CH}}$  vs.  $^1\text{D}_{\text{CC}}$  yields a slope,

$$m = (\gamma_{\text{H}}/\gamma_{\text{C}})\langle P_2(\cos\beta) \cdot r_{\text{CH}}^{-3} \rangle / \langle r_{\text{CC}}^{-3} \rangle, \quad (7)$$

where  $\gamma_{\text{H}}$  and  $\gamma_{\text{C}}$  are the gyromagnetic ratios of  $^1\text{H}$  and  $^{13}\text{C}$ ,  $r_{\text{CC}}$  is the length of the  $\text{C}_{\text{methyl}}\text{-C}$  bond and  $P_2(\cos\beta)$  and  $r_{\text{CH}}$  are as defined previously (Ottiger and Bax, 1999). In their applications the molecule of interest was fully protonated. Since the goal of the present work is to study how  $\beta$  varies with deuterium substitution, measurements must be performed on fractionally deuterated proteins, complicating the experiments that are required. Each methyl deuteron leads to upfield shifts (-0.3 ppm per  $^2\text{H}$ ) of the carbon and the remaining protons (-0.02 ppm per  $^2\text{H}$ ) so that separate correlations are observed for each methyl isotopomer (Gardner et al., 1997). The presence of three components for each methyl can lead to overlap in correlation spectra and we have therefore developed a set of experiments for measuring  $^1\text{H}_{\text{methyl}}\text{-}^{13}\text{C}_{\text{methyl}}$  dipolar couplings which select only one of the three methyl isotopomers per experiment. The [ $^1\text{H}\text{-}^{13}\text{C}$ ] CT-HSQC based pulse schemes used for  $^{13}\text{CH}_3$ ,  $^{13}\text{CH}_2\text{D}$  and  $^{13}\text{CHD}_2$  methyl group selection are shown in Figure 1a ( $^{13}\text{CH}_3$ ) and 1b ( $^{13}\text{CH}_2\text{D}$ ,  $^{13}\text{CHD}_2$ ). In a similar manner it is straightforward to obtain separation of  $^{13}\text{CH}_3/^{13}\text{CHD}_2$  and  $^{13}\text{CH}_2\text{D}$  methyl isotopomers in experiments for measuring  $^{13}\text{C}_{\text{methyl}}\text{-}^{13}\text{C}$  dipolar couplings, as described in Materials and Methods, and in Mittermaier and Kay (1999). In what follows a brief description of the schemes for measuring  $^1\text{H}_{\text{methyl}}\text{-}^{13}\text{C}_{\text{methyl}}$  couplings is presented.

In the pulse scheme of Figure 1a magnetization is transferred from the methyl proton to the directly attached carbon so that at point *a* in the scheme the signal of interest is proportional to  $2C_y I_z$ , where  $C_y$  and  $I_z$  are the *y* and *z* components of  $^{13}\text{C}$  and  $^1\text{H}$  magnetization, respectively. During the subsequent period of duration  $2T_{\text{C}}$ , ( $2T_{\text{C}} = 1/J_{\text{CC}}$ , where  $J_{\text{CC}}$  is the one-bond  $^{13}\text{C}\text{-}^{13}\text{C}$  scalar coupling) extending from points *a* to *b*, magnetization derived from methyl isotopomers  $^{13}\text{CH}_2\text{D}$  and  $^{13}\text{CHD}_2$  is reduced by applying

a  $^2\text{H}$   $90^\circ$  purge pulse at a time  $T_{\text{C}} \sim 1/(4J_{\text{CD}})$  (Gardner et al., 1997). This pulse creates  $^{13}\text{C}\text{-}^2\text{H}$  double and zero quantum coherences which are dephased by the subsequent gradient pulses. Additionally,  $^2\text{H}$  spin flips attenuate correlations derived from deuterium containing methyl groups still further (Grzesiek et al., 1993). A second  $^2\text{H}$  purge pulse is inserted at a time  $\tau_{\text{c}} = 1/(4J_{\text{CD}})$  after point *c*, again eliminating signal arising from these isotopomers. Thus, a 2D  $^{13}\text{C}\text{-}^1\text{H}$  correlation spectrum is obtained (Figure 2a) containing contributions from  $\text{CH}_3$  isotopomers only. A series of spectra is recorded as a function of  $t_1$  and the intensity of the correlations fit to Equation 2 to obtain values for  $^1J_{\text{CH}} + ^1\text{D}_{\text{CH}}$  (aligned sample) or  $^1J_{\text{CH}}$  (no alignment);  $^1\text{D}_{\text{CH}}$  is calculated from the difference in couplings measured in the presence and absence of aligning media.

The pulse scheme used to select  $\text{CH}_2\text{D}$  isotopomers is shown in Figure 1b (with  $\varphi_2 = \varphi_5 = x$  and the  $^1\text{H}$   $90^\circ$  pulse in parenthesis eliminated). The elements between points *a* and *b* [ $2\tau_b \approx 1/(2 \cdot ^1J_{\text{CH}})$ ] and again between *c* and *d* [ $2\tau'_b \approx (2 \cdot ^1J_{\text{CH}})$ ] are used as purges to eliminate signal arising from the undesired isotopomers. For example, if the one-bond  $^{13}\text{C}\text{-}^1\text{H}$  coupling is uniform then the delay  $2\tau_b$  can be adjusted so that the signal at point *b* is proportional to  $C_x$ ,  $2C_y I_z$ ,  $4C_x I_z I_z$  for  $^{13}\text{CHD}_2$ ,  $^{13}\text{CH}_2\text{D}$  and  $^{13}\text{CH}_3$  methyl types; the action of the subsequent carbon pulse and gradient ensures that only terms of the form  $2C_y I_z$  survive. In the case of alignment  $^1\text{H}\text{-}^{13}\text{C}$  couplings vary somewhat and it is not possible to select a single  $\tau_b$  value which ensures that  $\text{CH}_3$  and  $\text{CHD}_2$  isotopomers are completely purged. For this reason  $\tau_b$  and  $\tau'_b$  are chosen to be of slightly different durations. Figure 2b shows a portion of the correlation spectrum, illustrating that only methyls of the  $\text{CH}_2\text{D}$  type have been selected. As described above, a set of spectra are recorded and cross-peak intensities fit to Equation 3 with  $n = 2$  to obtain coupling values.

The pulse scheme of Figure 2b can also be used to select for  $\text{CHD}_2$  methyl groups so long as  $\varphi_2 = \varphi_5 = y$  and in this case the  $^1\text{H}$   $90^\circ$  pulse in parenthesis is applied. Although correlations arising from  $\text{CH}_2\text{D}$  methyls are eliminated, as expected, we have not found it possible to completely suppress contributions from  $\text{CH}_3$  methyl groups. As described above  $^1\text{H}\text{-}^{13}\text{C}$  dipole-dipole cross-correlation effects are significant in methyl groups and evolution from the one-bond  $^1\text{H}\text{-}^{13}\text{C}$  coupling and cross-correlation during each of the two purging elements can lead to signals from fully protonated methyls, even if all delays are op-

timized for purging (Ishima et al., 1999). Figure 2c shows, however, that the cross-peaks arising from CH<sub>3</sub> methyls are weak (compare 2a with 2c); these extra correlations did not interfere with quantitation of <sup>1</sup>H-<sup>13</sup>C couplings from CHD<sub>2</sub> methyl groups in the present study. Intensities of peaks arising from CHD<sub>2</sub> methyl groups are obtained as a function of t<sub>1</sub> and fit to Equation 3 with n=1 to obtain <sup>1</sup>H-<sup>13</sup>C coupling values.

Figure 3 shows cross-peak intensity profiles for the δ2 methyl of Leu56 of protein L in isotropic media as a function of <sup>1</sup>H-<sup>13</sup>C coupling evolution delay, t<sub>1</sub>. As expected each of the different methyl isotopomers [(a) CH<sub>3</sub>, (b) CH<sub>2</sub>D and (c) CHD<sub>2</sub>] has a different profile. Best fit intensity profiles calculated according to Equations 2–3 are indicated by solid lines and reproduce the measured peak volumes (circles) very well. Scalar coupling values obtained from fits such as these are listed by residue and isotopomer in Table 1. Out of the 33 well resolved methyl correlations observed in 2D <sup>1</sup>H-<sup>13</sup>C maps of protein L data from 30 methyls have been used in what follows. The δ1 carbons of Leu38 and Leu56 are strongly coupled to their adjacent γ carbons and were therefore not included in any analysis. In addition, the <sup>1</sup>D<sub>CH</sub>:<sup>1</sup>D<sub>CC</sub> ratio for the γ1 methyl group of Val2 is uncharacteristically large, possibly due to distorted local geometry (see below). Data for this methyl group was also omitted. Figure 3d shows the cross-peak intensity profile for the Leu56 δ2 methyl (protein L) as a function of the <sup>13</sup>C-<sup>13</sup>C coupling delay, T (isotropic phase). One bond <sup>13</sup>C<sub>methyl</sub>-<sup>13</sup>C scalar couplings extracted from fits of profiles of this sort have been tabulated in Table 2.

Table 1 shows that there are clear substituent effects on one-bond <sup>1</sup>H-<sup>13</sup>C scalar couplings, with <sup>1</sup>J<sub>CH</sub> values decreasing with increasing aliphatic character of the residue. The one bond <sup>1</sup>H<sub>methyl</sub>-<sup>13</sup>C<sub>methyl</sub> scalar coupling is largest for alanine (130.0 ± 0.6 Hz) and smallest for leucine residues (124.5 ± 0.8 Hz). As well, there is a small yet significant isotope dependence with values on average 0.16 Hz larger in CH<sub>3</sub> relative to CH<sub>2</sub>D and 0.36 Hz larger in CH<sub>2</sub>D relative to CHD<sub>2</sub> when scalar couplings for the same methyl group are compared. Values for ⟨Δ<sup>1</sup>J<sub>CH</sub>⟩ are within 0.06 to 0.26 Hz at the 99% confidence level for ⟨<sup>1</sup>J<sub>CH</sub><sup>CH<sub>3</sub></sup> - <sup>1</sup>J<sub>CH</sub><sup>CH<sub>2</sub>D}</sup>⟩, within 0.30 to 0.43 Hz for ⟨<sup>1</sup>J<sub>CH</sub><sup>CH<sub>2</sub>D}</sup> - <sup>1</sup>J<sub>CH</sub><sup>CHD<sub>2</sub>}</sup>⟩ and within 0.38 to 0.67 Hz for ⟨<sup>1</sup>J<sub>CH</sub><sup>CH<sub>3</sub>}</sup> - <sup>1</sup>J<sub>CH</sub><sup>CHD<sub>2</sub>}</sup>⟩. The probabilities that the observed differences in scalar couplings could arise purely from random effects are 1.5 × 10<sup>-4</sup>, 4.8 × 10<sup>-16</sup> and 4.6 × 10<sup>-11</sup> for differ-

ences in couplings in CH<sub>3</sub>,CH<sub>2</sub>D, CH<sub>2</sub>D,CHD<sub>2</sub> and CH<sub>3</sub>,CHD<sub>2</sub> isotopomer pairs, respectively. This trend has been observed experimentally in methane (Bennett et al., 1989) with <sup>1</sup>J<sub>CH</sub> values of 125.31, 124.95 and 124.26 Hz reported for <sup>13</sup>CH<sub>4</sub>, <sup>13</sup>CH<sub>3</sub>D and <sup>13</sup>CHD<sub>3</sub>, respectively. *Ab initio* calculations of <sup>1</sup>J<sub>CH</sub> as a function of deuteration in methane (Wigglesworth et al., 1997) also show the same trend and indicate that the shorter length of the CD bond translates into a slight increase in the remaining CH bonds, with a concomitant decrease in <sup>1</sup>H-<sup>13</sup>C scalar couplings.

Table 2 shows that substituent effects have a smaller influence on the values of <sup>1</sup>J<sub>CC</sub> than on <sup>1</sup>J<sub>CH</sub>. Only in the case of threonine are elevated <sup>13</sup>C<sub>methyl</sub>-<sup>13</sup>C scalar couplings observed relative to values obtained for other methyl containing residues. Similar to what has been observed with <sup>1</sup>J<sub>CH</sub>, <sup>1</sup>J<sub>CC</sub> scalar couplings are found to decrease with increasing methyl deuterium content. Average differences are smaller than for proton-carbon couplings with <sup>1</sup>J<sub>CC</sub> on average 0.072 Hz larger in C-CH<sub>3</sub> methyls relative to C-CH<sub>2</sub>D groups and 0.060 Hz larger in C-CH<sub>2</sub>D relative to C-CHD<sub>2</sub> methyl isotopomers. The statistical significance of these deviations are comparable to what has been noted for <sup>1</sup>J<sub>CH</sub> values above, with p = 2.0 × 10<sup>-12</sup>, 1.3 × 10<sup>-8</sup> and 4.1 × 10<sup>-13</sup> for CH<sub>3</sub>-CH<sub>2</sub>D, CH<sub>2</sub>D-CHD<sub>2</sub> and CH<sub>3</sub>-CHD<sub>2</sub> isotopomer pairs, respectively.

Figure 4a shows the correlations obtained between measured <sup>1</sup>D<sub>CH</sub> and <sup>1</sup>D<sub>CC</sub> values for the different methyl isotopomers. Values for ⟨P<sub>2</sub>(cos β) · r<sub>CH</sub><sup>-3</sup>⟩ can be readily calculated from the slopes of the correlations, using Equation 7 above. In all three cases the uncertainties in the slopes were assessed using bootstrap methods giving ranges indicated by the shaded regions in Figure 4a. The bracketed point corresponds to the γ1 methyl of Val2, and was not included in the fits. Using r<sub>CC</sub> = 1.517 Å (Engh & Huber, 1991) and γ<sub>H</sub>/γ<sub>C</sub> = 3.976 (Cavanagh et al., 1996), mean values of ⟨P<sub>2</sub>(cos β) · r<sub>CH</sub><sup>-3</sup>⟩ were obtained for CH<sub>3</sub> (-0.228 ± 0.003 Å<sup>-3</sup>), CH<sub>2</sub>D (-0.225 ± 0.004 Å<sup>-3</sup>) and CHD<sub>2</sub> (-0.223 ± 0.004 Å<sup>-3</sup>) by averaging over all bootstrap iterations. It is worth mentioning that the value of -0.228 Å<sup>-3</sup> obtained for CH<sub>3</sub> isotopomers using the methodology described herein is in excellent agreement with the value that has been reported by Ottiger and Bax in their previous study (-0.228).

Assuming an effective CH bond length of 1.117 Å, as suggested by Ottiger and Bax (1998) for the C<sup>α</sup>-H<sup>α</sup> bond ((r<sub>CH</sub><sup>-3</sup>)<sup>-1/3</sup>; this value includes the effects of librations) average β values of 110.4°, 110.7° and 110.8° are calculated for CH<sub>3</sub>, CH<sub>2</sub>D and CHD<sub>2</sub>

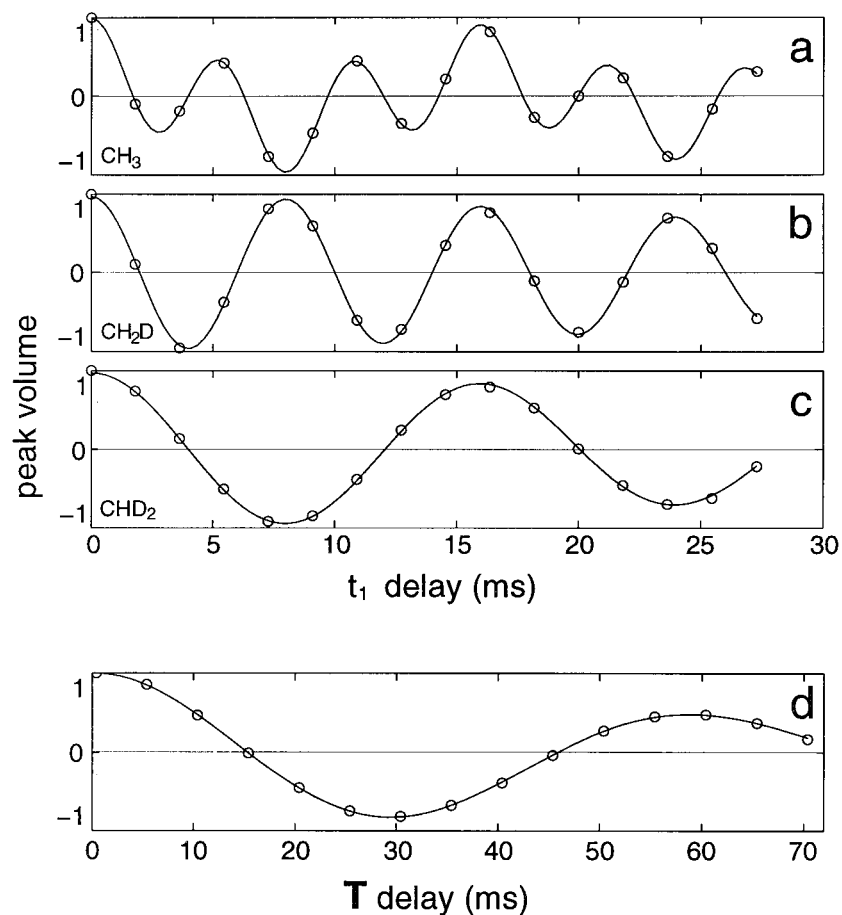


Figure 3. Time dependence of the  $\delta 2$  methyl cross-peak intensity for Leu56 in the B1 domain of protein L (isotropic sample) due to evolution from the one-bond  $^1\text{H}$ - $^{13}\text{C}$  coupling obtained from (a)  $\text{CH}_3$ , (b)  $\text{CH}_2\text{D}$  and (c)  $\text{CHD}_2$  selective experiments and from evolution due to the  $^{13}\text{C}_{\text{methyl}}$ - $^{13}\text{C}$  coupling (d,  $\text{CH}_2\text{D}$  selective experiment (Mittermaier and Kay, 1999; Muhandiram et al., 1995)). The solid lines correspond to best fit curves using Equations 1–3 in the text.

Table 1. One bond  $^1\text{H}$ - $^{13}\text{C}$  scalar couplings (Hz)

Methyl	$\text{CH}_3$		$\text{CH}_2\text{D}$		$\text{CHD}_2$		$N^{\text{d}}$
	Mean <sup>a</sup>	St dev <sup>a</sup>	Mean <sup>b</sup>	St dev <sup>b</sup>	Mean <sup>c</sup>	St dev <sup>c</sup>	
Ala $\beta$	130.0	0.6	129.7	0.6	129.4	0.6	9
Thr $\gamma 2$	127.3	0.4	127.2	0.4	126.8	0.4	6
Val $\gamma 1,2$	126.2	0.3	126.1	0.3	125.6	0.3	5
Ile $\gamma 2$	126.2	0.0	126.0	0.1	125.6	0.1	3
Ile $\delta 1$	125.2	0.3	125.1	0.4	124.6	0.2	3
Leu $\delta 1,2$	124.5	0.8	124.7	0.5	124.4	0.4	4

<sup>a</sup>Mean and standard deviation of  $^1J_{\text{CH}}$  values obtained from fits to Equation 2 using  $\text{CH}_3$  derived data and an unaligned sample.

<sup>b</sup>Mean and standard deviation of  $^1J_{\text{CH}}$  values obtained from fits to Equation 3 with  $n=2$  using  $\text{CH}_2\text{D}$  derived data and an unaligned sample.

<sup>c</sup>Mean and standard deviation of  $^1J_{\text{CH}}$  values obtained from fits to Equation 3 with  $n=1$  using  $\text{CHD}_2$  derived data and an unaligned sample.

<sup>d</sup>Number of scalar coupling values obtained for each methyl type (omitting Leu38 $\delta$ 1, Leu56 $\delta$ 1 and Val2 $\gamma$ 1).



Table 2. One bond  $^{13}\text{C}$ - $^{13}\text{C}$  scalar couplings (Hz)

Methyl	$\text{CH}_3$		$\text{CH}_2\text{D}$		$N^c$	$\text{CHD}_2$		$N^e$
	Mean <sup>a</sup>	St dev <sup>a</sup>	Mean <sup>b</sup>	St dev <sup>b</sup>		Mean <sup>d</sup>	St dev <sup>d</sup>	
Ala $\beta$	34.2	0.8	34.1	0.8	9	34.0	0.9	8
Thr $\gamma_2$	38.3	1.0	38.3	1.0	6	38.1	1.1	5
Val $\gamma_{1,2}$	35.0	0.3	34.9	0.3	5	34.9	0.3	4
Ile $\gamma_2$	35.0	0.2	35.0	0.2	3	34.9	0.2	3
Ile $\delta_1$	34.8	0.3	34.7	0.2	3	34.6	0.2	3
Leu $\delta_{1,2}$	34.3	0.6	34.2	0.6	4	34.1	0.6	4

<sup>a</sup>Mean and standard deviation of  $^1J_{\text{CC}}$  values obtained from fits to Equation 1 using  $\text{CH}_3$  derived data and an unaligned sample.

<sup>b</sup>Mean and standard deviation of  $^1J_{\text{CC}}$  values obtained from fits to Equation 1 using  $\text{CH}_2\text{D}$  derived data and an unaligned sample.

<sup>c</sup>Number of scalar coupling values obtained for  $\text{CH}_3$  and  $\text{CH}_2\text{D}$  methyls (omitting Leu38 $\delta_1$ , Leu56 $\delta_1$  and Val2 $\gamma_1$ ).

<sup>d</sup>Mean and standard deviation of  $^1J_{\text{CC}}$  values obtained from fits to Equation 1 using  $\text{CHD}_2$  derived data and an unaligned sample.

<sup>e</sup>Number of scalar coupling values obtained for  $\text{CHD}_2$  methyls (omitting Leu38 $\delta_1$ , Leu56 $\delta_1$  Val2 $\gamma_1$ , Ala50 $\beta$ , Thr3 $\gamma_2$  and Val49 $\gamma_1$ ).

methyl types from the values of  $\langle P_2(\cos \beta) \cdot r_{\text{CH}}^{-3} \rangle$  obtained from the slopes in Figure 4a. To assess whether the differences in these values are significant, 100 000  $\beta$  values have been calculated for each methyl type using the bootstrap approach described in Materials and Methods. Differences in  $\beta$ ,  $\Delta\beta$ , obtained for each pair of methyl isotopomers have been used to calculate distribution functions for the true values of  $\Delta\beta$ , shown in Figure 4b. It is clear that a substantial fraction of each distribution is on both sides of 0 (that is the differences in  $\Delta\beta$  values are of marginal statistical significance). In fact, 95.4% ( $\Delta\beta^{\text{CH}_3-\text{CH}_2\text{D}}$ ), 71.9% ( $\Delta\beta^{\text{CH}_2\text{D}-\text{CHD}_2}$ ) and 93.1% ( $\Delta\beta^{\text{CH}_3-\text{CHD}_2}$ ) of the distributions are less than 0° corresponding to a one-tailed statistical significance (p) of 4.6%, 28.1% and 6.9% for  $\Delta\beta^{\text{CH}_3-\text{CH}_2\text{D}}$ ,  $\Delta\beta^{\text{CH}_2\text{D}-\text{CHD}_2}$  and  $\Delta\beta^{\text{CH}_3-\text{CHD}_2}$ , respectively. A maximum deviation at the 99% confidence level of  $-1.04^\circ$  is obtained for  $\Delta\beta^{\text{CH}_3-\text{CHD}_2}$ ; for  $\Delta\beta^{\text{CH}_3-\text{CH}_2\text{D}}$  the largest difference is  $-0.59^\circ$ . In order to further establish the significance of differences in  $\beta$  as a function of isotopomers, an additional statistical test was applied. In the absence of any changes in the angle  $\beta$ , a plot of  $^1D_{\text{CH}}$  values from one isotopomer vs. the corresponding values from another should yield a slope of one. In fact, slopes of  $0.986 \pm 0.006$ ,  $0.990 \pm 0.014$  and  $0.976 \pm 0.015$  are obtained for  $^1D_{\text{CH}}^{\text{CH}_3}$  vs.  $^1D_{\text{CH}}^{\text{CH}_2\text{D}}$ ,  $^1D_{\text{CH}}^{\text{CH}_2\text{D}}$  vs.  $^1D_{\text{CH}}^{\text{CHD}_2}$  and  $^1D_{\text{CH}}^{\text{CH}_3}$  vs.  $^1D_{\text{CH}}^{\text{CHD}_2}$ , respectively. The probabilities that slopes as small or smaller than these could be obtained if the true slope were unity, given the exper-

imental uncertainties in slopes, are 1.9%, 24.4% and 6.7% (see Materials and methods) in good agreement with bootstrap results above.

Changes in time-averaged geometry in response to deuterium substitution have been reported for theoretical calculations in methane (Raynes et al., 1988) with  $\langle \beta \rangle$  decreasing by 0.02 deg and  $\langle r_{\text{CH}} \rangle$  increasing by 1.5 parts in 10,000 when comparing  $\text{CH}_3\text{D}$  to  $\text{CH}_4$ . The differences in  $\beta$  are about 10-fold smaller than those obtained in this study:  $-0.25^\circ$  and  $-0.12^\circ$  for  $\text{CH}_3-\text{CH}_2\text{D}$  and  $\text{CH}_2\text{D}-\text{CHD}_2$ , respectively, yet lie within the 99% confidence regions of the  $\Delta\beta$  profiles reported here.

## Concluding remarks

Changes in structural parameters of methyl groups important in the analysis of  $^{13}\text{C}$  spin relaxation data have been investigated as a function of deuterium substitution. In particular, a comparison of  $^1J_{\text{CH}}$ ,  $^1J_{\text{CC}}$  values as a function of deuteration is presented along with a comparison of one bond  $^1\text{H}-^{13}\text{C}$  dipolar couplings with  $^{13}\text{C}_{\text{methyl}}-^{13}\text{C}$  dipolar couplings, measured on a per-methyl, per-isotopomer basis in a uniformly  $^{15}\text{N}$ ,  $^{13}\text{C}$ , randomly  $\sim 50\%$   $^2\text{H}$  labeled protein. Both  $^1J_{\text{CH}}$  and  $^1J_{\text{CC}}$  scalar couplings decrease with increasing deuteration levels, consistent, in the case of  $^1J_{\text{CH}}$ , with a lengthening of the methyl  $^1\text{H}-^{13}\text{C}$  bond. Average values of  $110.4^\circ$  ( $\text{CH}_3$ ),  $110.7^\circ$  ( $\text{CH}_2\text{D}$ ) and  $110.8^\circ$  ( $\text{CHD}_2$ ) for the  $\text{H}_{\text{methyl}}\text{C}_{\text{methyl}}\text{C}$

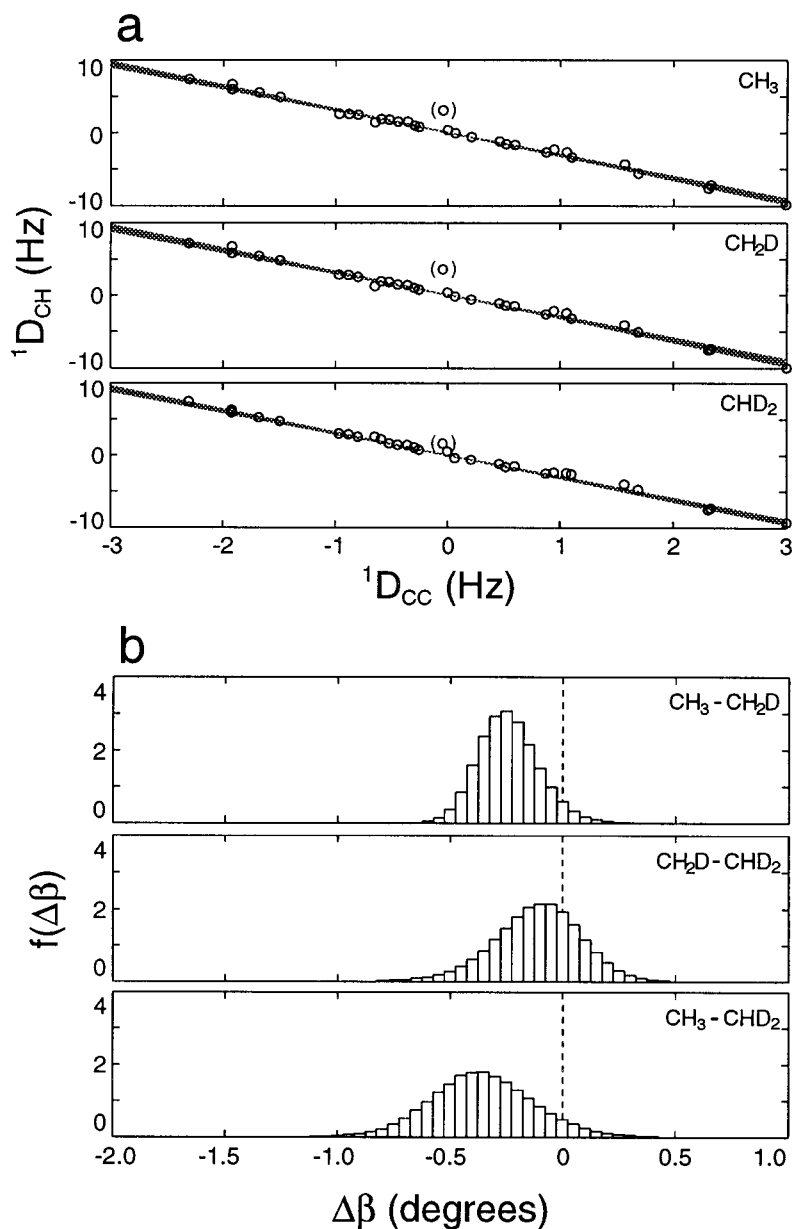


Figure 4. Plots of  $^1D_{CH}$  vs.  $^1D_{CC}$  residual dipolar couplings measured for methyl groups in the B1 domain of protein L aligned using Pf1 phage (a). Shaded regions indicate the range of linear fits through the origin obtained from bootstrap analysis. The bracketed point corresponds to the  $\gamma_1$  methyl of Val2 and was not included in the fits. (b) Distribution functions,  $f(\Delta\beta)$ , for the true values of differences in  $\beta$  calculated from the slopes in (a) and Equation 7, assuming  $r_{CC} = 1.517 \text{ \AA}$  (Engh and Huber, 1991),  $\gamma_H/\gamma_C = 3.976$  (Cavanagh et al., 1996), and  $r_{CH} = 1.117 \text{ \AA}$  obtained from 100 000 bootstrap iterations.

angle,  $\beta$ , have been obtained based on the correlation between  $^1D_{CH}$  and  $^1D_{CC}$  couplings, assuming a  $^1H$ - $^{13}C$  bond length of  $1.117 \text{ \AA}$ , corresponding to a decrease in  $|\langle P_2(\cos\beta) \cdot r_{CH}^{-3} \rangle|$  of approximately 2% from  $CH_3$  to  $CHD_2$  isotopomers. The present results em-

phasize the exquisite sensitivity of scalar and dipolar couplings to small changes in structure.

## Acknowledgements

The authors thank Dr Dennis A. Torchia (NIH) for suggesting the problem and for many stimulating discussions. This work is supported by a grant from the Natural Sciences and Engineering Research Council of Canada.

## References

- Bennett, B., Raynes, W. and Anderson, C. (1989) *Spectrochimica Acta*, **45A**, 821–827.
- Cavanagh, J., Fairbrother, W., Palmer, A. and Skelton, N. (1996) In *Protein NMR Spectroscopy Principles and Practice*, Academic Press, Inc., San Diego.
- Delaglio, F., Grzesiek, S., Vuister, G.W., Zhu, G., Pfeifer, J. and Bax, A. (1995) *J. Biomol. NMR*, **6**, 277–293.
- Efron, B. and Tibshirani, R. (1986) *Stat. Sci.*, **1**, 54–77.
- Engh, R.A. and Huber, R. (1991) *Acta Crystallogr.*, **A47**, 392–400.
- Freeman, R., Kempell, S.P. and Levitt, M.H. (1980) *J. Magn. Reson.*, **38**, 453–479.
- Gardner, K.H., Rosen, M.K. and Kay, L.E. (1997) *Biochemistry*, **36**, 1389–1401.
- Geen, H. and Freeman, R. (1991) *J. Magn. Reson.*, **93**, 93–141.
- Grzesiek, S., Anglister, J., Ren, H. and Bax, A. (1993) *J. Am. Chem. Soc.*, **115**, 4369–4370.
- Hansen, M.R., Mueller, L. and Pardi, A. (1998) *Nat. Struct. Biol.*, **5**, 1065.
- Ishima, R., Louis, J. and Torchia, D. (1999) *J. Am. Chem. Soc.*, **121**, 11589–11590.
- Ishima, R., Petkova, A., Louis, J. and Torchia, D. (2001) *J. Am. Chem. Soc.*, **123**, 6164–6171.
- Janin, J., Miller, S. and Chothia, C. (1988) *J. Mol. Biol.*, **204**, 155–164.
- Kay, L.E., Bull, T.E., Nicholson, L.K., Griesinger, C., Schwalbe, H., Bax, A. and Torchia, D.A. (1992) *J. Magn. Reson.*, **100**, 538–558.
- LeMaster, D.M. and Kushlan, D.M. (1996) *J. Am. Chem. Soc.*, **118**, 9255–9264.
- Marion, D., Ikura, M., Tschudin, R. and Bax, A. (1989) *J. Magn. Reson.*, **85**, 393–399.
- Mittermaier, A. and Kay, L. (1999) *J. Am. Chem. Soc.*, **121**, 10608–10613.
- Mittermaier, A. and Kay, L. (2001) *J. Am. Chem. Soc.*, **123**, 6892–6903.
- Muhandiram, D.R., Yamazaki, T., Sykes, B.D. and Kay, L.E. (1995) *J. Am. Chem. Soc.*, **117**, 11536–11544.
- Nicholson, L.K., Kay, L.E., Baldissari, D.M., Arango, J., Young, P.E., Bax, A. and Torchia, D.A. (1992) *Biochemistry*, **31**, 5253–5263.
- Ottiger, M. and Bax, A. (1998) *J. Am. Chem. Soc.*, **120**, 12334–12341.
- Ottiger, M. and Bax, A. (1999) *J. Am. Chem. Soc.*, **121**, 4690–4695.
- Ottiger, M., Delaglio, F., Marquardt, J.L., Tjandra, N. and Bax, A. (1998) *J. Magn. Reson.*, **134**, 365–369.
- Palmer, A.G., Wright, P.E. and Rance, M. (1991) *Chem. Phys. Lett.*, **185**, 41–46.
- Press, W.H., Flannery, B.P., Teukolsky, S.A. and Vetterling, W.T. (1988) In *Numerical Recipes in C*, Cambridge University Press, Cambridge, pp. 490–494.
- Raynes, W., Fowler, P., Lazzarotti, P., Zanasi, R. and Grayson, M. (1988) *Mol. Phys.*, **64**, 143162.
- Scalley, M.L., Yi, Q., Gu, H., McCormack, A., Yates, J.R. and Baker, D. (1997) *Biochemistry*, **36**, 3373–3382.
- Shaka, A.J., Keeler, J., Frenkiel, T. and Freeman, R. (1983) *J. Magn. Reson.*, **52**, 335–338.
- Wigglesworth, R., Raynes, W., Sauer, S. and Oddershede, J. (1997) *Mol. Phys.*, **92**, 77–88.
- Zar, J.H. (1984a) In *Biostatistical Analysis*, Prentice-Hall Inc., Englewood Cliffs, NJ, pp. 97–121.
- Zar, J.H. (1984b) In *Biostatistical Analysis*, Prentice-Hall Inc., Englewood Cliffs, NJ, pp. 261–291.
- Zhu, G. and Bax, A. (1990) *J. Magn. Reson.*, **90**, 405–410.